Comparison of a hair bundle's spontaneous oscillations with its response to mechanical stimulation reveals the underlying active process

P. Martin*†, A. J. Hudspeth*‡, and F. Jülicher†

*Howard Hughes Medical Institute and Laboratory of Sensory Neuroscience, The Rockefeller University, 1230 York Avenue, New York, NY 10021-6399; and †Laboratoire Physico-Chimie Curie, Unité Mixte de Recherche 168, Institut Curie, 26 rue d'Ulm, F-75248 Paris Cedex 05, France

Contributed by A. J. Hudspeth, October 5, 2001

Hearing relies on active filtering to achieve exquisite sensitivity and sharp frequency selectivity. In a quiet environment, the ears of many vertebrates become unstable and emit one to several tones. These spontaneous otoacoustic emissions, the most striking manifestation of the inner ear's active process, must result from self-sustained mechanical oscillations of aural constituents. The mechanoreceptive hair bundles of hair cells in the bullfrog's sacculus have the ability to amplify mechanical stimuli and oscillate spontaneously. By comparing a hair bundle's spontaneous oscillations with its response to small mechanical stimuli, we demonstrate a breakdown in a general principle of equilibrium thermodynamics, the fluctuation–dissipation theorem. We thus confirm that a hair bundle's spontaneous movements are produced by energy-consuming elements within the hair cell. To characterize the dynamical behavior of the active process, we introduce an effective temperature that, for each frequency component, quantifies a hair bundle's deviation from thermal equilibrium. The effective temperature diverges near the bundle's frequency of spontaneous oscillation. This behavior, which is not generic for active oscillators, can be accommodated by a simple model that characterizes quantitatively the fluctuations of the spontaneous movements as well as the hair bundle's linear response function.

The vertebrate ear not only admits but also *emits* sound. In amphibians, reptiles, birds, and mammals, microphone recordings in a quiet environment disclose one to several tones emerging from normal ears (reviewed in refs. 1–3). These spontaneous otoacoustic emissions (SOAEs) are sometimes so loud that they may be heard at a distance (4). Because the emission of sound requires power, SOAEs must be generated by a work-producing process.

Otoacoustic emissions represent the most striking manifestation of an active process in the inner ear. Even before SOAEs were observed, it was recognized that hearing must use an energy source to overcome the damping effect of the inner ear's fluid on movements of the basilar membrane and other aural constituents (5). The ear's exquisite sensitivity and sharp frequency selectivity for minute stimuli result from this active process (reviewed in refs. 6, 7). Theoretical analysis reveals that many of the characteristic phenomena observed in hearing can be produced by an active system operating at the onset of an oscillatory instability, the Hopf bifurcation (8–10). A self-tuning mechanism likely maintains the ear's active components near the instability, thereby ensuring that the organ's sensitivity and frequency selectivity are optimal (9). In a quiet environment, unprovoked oscillations by the active process manifest themselves as SOAEs.

Two forms of cellular motility have been proposed to underlie the inner ear's active process. Extensive research on mammals argues that electrically driven cell–body movements of specialized mechanoreceptors, the outer hair cells, provide the work required of the active process (reviewed in refs. 11–13). Nonmammalian tetrapods, however, lack outer hair cells and probably the associated process of electromotility. In amphibians, reptiles, and birds, the best candidate for an active process is active motility of the mechanically sensitive hair bundles (reviewed in refs. 14–16).

If hair bundles mediate the active process, they must be capable of producing the energetic movements that underlie SOAEs. In the ears of reptiles and amphibians, hair bundles do have the ability to oscillate spontaneously (17–22). The magnitude of this hair-bundle motion can be severalfold as great as expected for the action of thermal noise on a structure of the stiffness that the bundle manifests during large displacements (23). It was initially argued on this basis that the bundle's motion violates the equipartition theorem and is therefore active, requiring a cellular energy source (17–19). It is now recognized, however, that a hair bundle's stiffness is a nonlinear function of displacement (22, 24–26). For saturating displacements greater than a few tens of nanometers, the bundle's stiffness is ~ 1 $\mathrm{mN \cdot m^{-1}}$. Over the range of displacements in which transduction channels open and close, the stiffness declines, an effect that can reduce the bundle's overall stiffness to zero or even render it negative (22). This observation raises the question whether a hair bundle's spontaneous movements are truly active, or whether they represent thermal fluctuations of an extraordinarily compliant structure.

Without specific knowledge of the underlying physical mechanism, how can one determine whether the spontaneous motions of *any* mechanical system are active or passive? When a passive system is at thermal equilibrium with its environment, its behavior must be constrained by the laws of thermodynamics. The system's spontaneous fluctuations then bear a specific relation at all frequencies to its responsiveness to small external stimuli. Violation of this correspondence constitutes proof that the system is active. In the present study, we have applied this reasoning to examine the basis of spontaneous oscillation by hair bundles.

Materials and Methods

Experimental Procedures. In each experiment, the saccular macula was dissected from the internal ear of an adult bullfrog (*Rana catesbeiana*) and secured in a two-compartment experimental chamber, as described previously (21). The basolateral surfaces of the hair cells were exposed to standard saline solution,

Abbreviations: FDT, fluctuation-dissipation theorem; SOAE, spontaneous otoacoustic emission.

‡To whom reprint requests should be addressed. E-mail: hudspaj@rockvax.rockefeller.edu.

The publication costs of this article were defrayed in part by page charge payment. This article must therefore be hereby marked "*advertisement*" in accordance with 18 U.S.C. §1734 solely to indicate this fact.

whereas their hair bundles projected into NMDG artificial endolymph. This arrangement mimicked the ionic circumstances *in vitro*, in particular by imposing a low Ca^{2+} concentration around the hair bundles.

Details of the techniques for mechanical stimulation, imaging, and optical calibration have been published (20, 21). The tip of a flexible glass fiber ~100 μm in length and ~0.5 μm in diameter was attached to the kinociliary bulb of an individual hair bundle. The fiber served both to report the hair bundle's position and to exert forces at its top. The image of the fiber's tip was projected at a magnification of ×1,000 onto a pair of photodiodes, by means of which the position of the tip and the attached bundle was monitored with a resolution of ~1 nm. We used a piezoelectric actuator to stimulate the hair bundle by displacing the fiber's base. To calibrate the stimulus force, we deduced the fiber's stiffness, $K_F = 250\ \mu N \cdot m^{-1}$, and its drag coefficient, $\xi = 120\ nN \cdot s \cdot m^{-1}$, from the spectrum of Brownian motion at the fiber's tip before attachment to a hair bundle.

Autocorrelation Function of Hair-Bundle Displacement. We denote by $X(t)$ the displacement of the hair bundle's top at its point of contact with the fiber. With its base held fixed, the fiber exerted no external force. We monitored the bundle's displacement relative to its mean position; this imposed the condition that $\langle X(t)\rangle = 0$. We then computed the autocorrelation function for spontaneous motion of the combined system of bundle and fiber, defined as

$$C(t) = \langle X(t + t_0)X(t_0)\rangle. \quad [1]$$

Independent of t_0, this function characterizes the stochastic properties of the displacement fluctuations. The power spectrum of the spontaneous motion is given by the Fourier transform of the autocorrelation function,

$$\tilde{C}(\omega) = \int_{-\infty}^{+\infty} C(t)e^{i\omega t}dt. \quad [2]$$

Hair-Bundle Response Function. We measured the average hair-bundle displacement, $\langle X(t)\rangle$, in response to a time-dependent stimulus that resulted from a sinusoidal displacement, $\Delta(t)$, of the fiber's base. For small stimulus amplitudes, the relation between these parameters was linear (27) and could be expressed as

$$\langle X(t)\rangle = \int_{-\infty}^{t} \Pi(t - t')\Delta(t')dt', \quad [3]$$

in which we have introduced the function $\Pi(t)$ to characterize the bundle's response to fiber displacements. Note that causality requires that $\Pi(t) = 0$ for $t < 0$. The Fourier representation of the frequency-dependent response function could be obtained as the dimensionless ratio

$$\tilde{\Pi}(\omega) = \frac{\langle \tilde{X}(\omega)\rangle}{\tilde{\Delta}(\omega)}. \quad [4]$$

$\tilde{\Pi}(\omega)$ was estimated at various frequencies by imposing sinusoidal stimuli on the hair bundle.

A second response function, $\chi(t)$, characterizes the response of the combined system of a hair bundle attached to a fiber to an external force, $f(t)$, applied at the bundle's top with the fiber's base held at a fixed position:

$$\langle X(t)\rangle = \int_{-\infty}^{t} \chi(t - t')f(t')dt'. \quad [5]$$

Although we did not actually apply the force $f(t)$, we can readily relate χ to the experimentally determined response function Π. As derived below, the spectral representation of $\chi(t)$ can be expressed as

$$\tilde{\chi}(\omega) = \frac{\tilde{\Pi}(\omega)}{K_F + i\omega\xi} \quad [6]$$

in which K_F and ξ represent respectively the stiffness and a drag coefficient of the fiber. Note that $\tilde{\chi}(\omega)$ has the units of a compliance.

Effect of Viscous Drag on the Fiber. The force $f_F(t)$ exerted on the hair bundle by the fiber had both elastic and viscous components. For small displacements, a linear approximation of $f_F(t)$ yields

$$f_F(t) = K_F[\Delta(t) - X(t)] - \xi_{XX}\frac{dX(t)}{dt} - \xi_{\Delta X}\frac{d\Delta(t)}{dt}, \quad [7]$$

in which we have introduced the two drag coefficients ξ_{XX} and $\xi_{\Delta X}$. The coefficient ξ_{XX} characterizes the viscous force on the hair bundle when the fiber's tip moves while its base is stationary. Similarly, $\xi_{\Delta X}$ characterizes the viscous force on the bundle owing to motion of the fiber's base while its tip is held fixed.

To relate the response function $\chi(t)$ of the combination of the bundle and fiber to the experimentally measured function $\Pi(t)$ (Eq. **6**), we first introduce the hair-bundle response function $\chi_{HB}(t)$, which characterizes the response to external forces of the bundle alone. In the presence of a fiber fixed at its base and with an external force $f(t)$ acting at the bundle's top, we have

$$\langle \tilde{X}(\omega)\rangle = \tilde{\chi}(\omega)\tilde{f}(\omega) = \tilde{\chi}_{HB}(\omega)[(-K_F + i\omega\xi_{XX})\langle \tilde{X}(\omega)\rangle + \tilde{f}(\omega)]. \quad [8]$$

We thus obtain a relation between $\tilde{\chi}_{HB}(\omega)$ and $\tilde{\chi}(\omega)$:

$$\tilde{\chi}(\omega) = \frac{\tilde{\chi}_{HB}(\omega)}{1 + \tilde{\chi}_{HB}(\omega)[K_F - i\omega\xi_{XX}]}. \quad [9]$$

Moreover, for the situation in which we apply a stimulus by moving the fiber's base sinusoidally at angular frequency ω,

$$\begin{aligned}\langle \tilde{X}(\omega)\rangle &= \tilde{\Pi}(\omega)\tilde{\Delta}(\omega) \\ &= \tilde{\chi}_{HB}(\omega)[(-K_F + i\omega\xi_{XX})\langle \tilde{X}(\omega)\rangle + (K_F + i\omega\xi_{\Delta X})\tilde{\Delta}(\omega)]\end{aligned} \quad [10]$$

and therefore

$$\tilde{\Pi}(\omega) = \frac{\tilde{\chi}_{HB}(\omega)[K_F + i\omega\xi_{\Delta X}]}{1 + \tilde{\chi}_{HB}(\omega)[K_F - i\omega\xi_{XX}]}. \quad [11]$$

Comparison of Eqs. **9** and **11** leads to

$$\tilde{\chi}(\omega) = \frac{\tilde{\Pi}(\omega)}{K_F + i\omega\xi_{\Delta X}} \quad [12]$$

The imaginary part $\tilde{\chi}''(\omega)$ of the response function $\tilde{\chi}(\omega)$ can be deduced from the observed function $\tilde{\Pi}(\omega)$ through the relation

$$\tilde{\chi}''(\omega) = \frac{-\omega\xi_{\Delta X}\tilde{\Pi}'(\omega) + K_F\tilde{\Pi}''(\omega)}{K_F^2 + \omega^2\xi_{\Delta X}^2}. \quad [13]$$

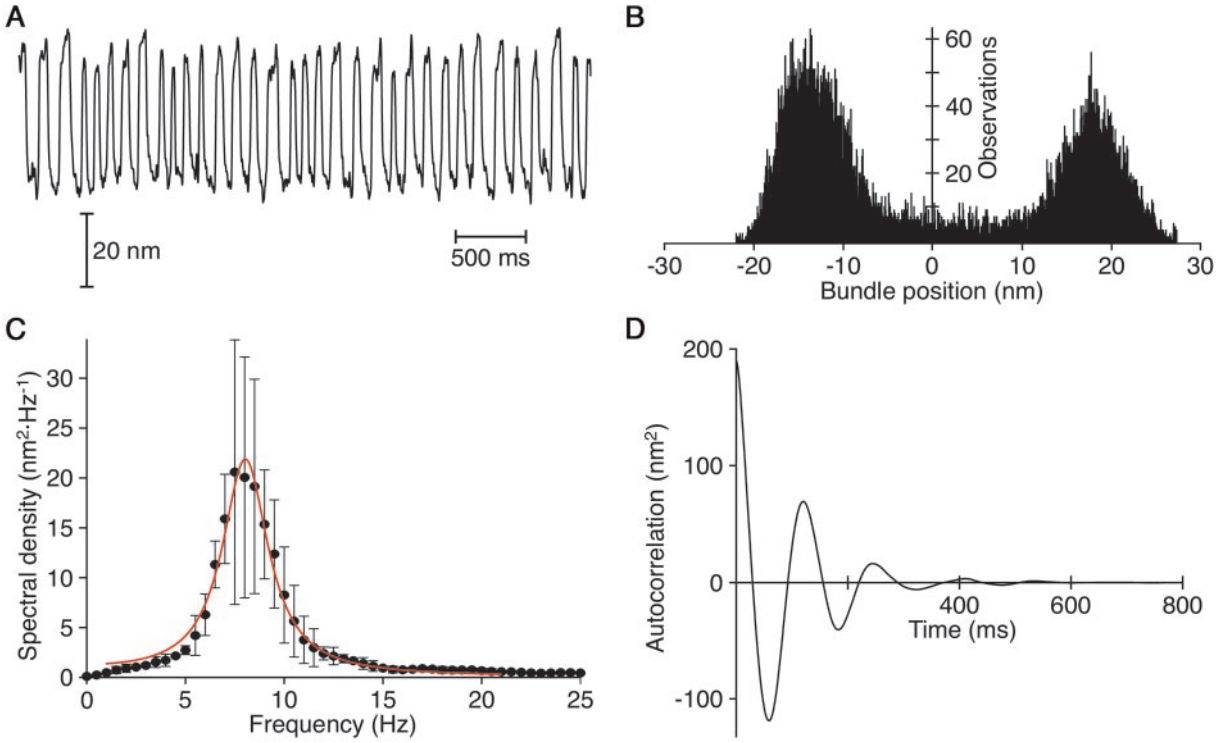

Fig. 1. Properties of spontaneous oscillations at ~8 Hz by a hair bundle from the sacculus of the bullfrog's inner ear. (*A*) Monitoring the position of a glass fiber attached at the hair bundle's top measured the bundle's spontaneous movement. This oscillation had a root–mean–square magnitude of 28 nm. The data were smoothed by forming the running average of a number of points equal to one-fifth of a cycle, and drift in the baseline was subtracted. (*B*) The probability distribution of bundle positions was bimodal, with a local minimum near the bundle's mean position. This histogram is asymmetrical; the bundle spent more time during negative than positive deflections. (*C*) The signal's spectrum displayed a broad peak and was fitted by Eq. **21** (smooth curve). We found $D = 0.14$ pN^2·s, $\lambda = 9$ μN·s·m^{-1}, $k = 80$ μN·m^{-1}, and $\nu_0 = \omega_0/(2\pi) = 8$ Hz; the ratio $\lambda/k = 115$ ms characterized the correlation time of the bundle's movements. To obtain the spectrum, we averaged the spectral densities computed from 15 measurements of bundle oscillations, each 2 s in length. The resulting spectrum was further smoothed by forming the running average of the number of points sampling a 1-Hz frequency band. The error bars specify standard deviations from these mean values. (*D*) The autocorrelation function of bundle motion, obtained as the inverse Fourier transform of the spectral density, revealed an average oscillation frequency of ~8 Hz. The signal's envelope, which relaxed towards zero with an exponential time constant of 115 ms, reflected the period over which the oscillation's phase lost coherence. Analog signals were sampled at a frequency of 2.5 kHz. *B*, *C*, and *D* derive from the data shown in *A*.

The value of the coefficient ξ_{XX} could be estimated from the Brownian motion of a free fiber's tip. The coefficient $\xi_{\Delta X}$, however, was more difficult to determine. We assumed for simplicity that the two coefficients were equal: $\xi_{\Delta X} \approx \xi \equiv \xi_{XX}$. Eq. **12** is then identical to Eq. **6**.

Results

Spontaneous Hair-Bundle Oscillations. When bathed in artificial endolymph, many of the ~2,500 hair bundles in the sensory epithelium of the bullfrog's sacculus oscillated spontaneously. As reported by the motion of a flexible fiber attached to the top of an oscillating hair bundle, the motion consisted of alternating slow components followed by fast strokes in the opposite direction (Fig. 1*A*). The probability distribution of the bundle's position was bimodal, with a local minimum near $X = 0$ (Fig. 1*B*). This distribution resembles that observed for sound pressure at the frequency of an SOAE from the human ear (28).

Hair-bundle movements fluctuated both in amplitude and in phase. To characterize these fluctuations, we computed the autocorrelation function $C(t) = \langle X(t)X(0)\rangle$ and its Fourier transform, $\tilde{C}(\omega)$, which defines the spectral density of bundle motion at each frequency $\nu = \omega/(2\pi)$. The spectral density peaked at a nonzero frequency, here $\nu_0 = 8$ Hz (Fig. 1*C*). The width of the function at half its maximal value, $\Delta\nu_0 = 2.8$ Hz, describes the frequency fluctuations around ν_0, which reflect a loss in phase coherence of the bundle oscillation. This property is clearly illustrated by the autocorrelation function (Fig. 1*D*): $C(t)$ assumes the form of a damped oscillation that decays toward zero with a correlation time $\tau = 1/(\pi\Delta\nu_0)$, 115 ms in this example.

Active vs. Passive Systems: The Fluctuation–Dissipation Theorem. Are these properties alone sufficient to determine whether spontaneous hair-bundle oscillations are generated by an active process? Stochastic displacements similar to those observed could in principle occur at equilibrium in a system buffeted by thermal forces. A definitive proof that the observed oscillation is active must invoke the breakdown of a general thermodynamic principle (29). The fluctuation–dissipation theorem (FDT) provides a useful instance of such a principle that assumes no physical properties of the system under investigation other than thermal equilibrium. The theorem asserts that the autocorrelation function of a passive system is directly related to the system's linear responsiveness $\chi(t)$ to small external forces. The relation may be written for $t > 0$ as

$$\chi(t) = -\frac{1}{k_B T}\frac{dC(t)}{dt}, \qquad [14]$$

in which k_B is the Boltzmann constant and T the temperature (reviewed in ref. 30).

The Fourier representation of Eq. **14** leads to

$$\tilde{C}(\omega) = 2k_B T\frac{\tilde{\chi}''(\omega)}{\omega}. \qquad [15]$$

Here $\tilde{\chi}''(\omega)$ is the imaginary or dissipative part of the frequency-dependent response function. In the case of a constant force $f(t) = f_0$, the combination of the FDT with the definition of the response function (Eq. **5**) yields

$$\langle X \rangle = \frac{\langle X^2 \rangle}{k_B T} f_0. \qquad [16]$$

The FDT thus ensures that the equipartition theorem is satisfied: $\frac{1}{2}\mathrm{K}\langle X^2 \rangle = \frac{1}{2}k_B T$, in which $\mathrm{K} = f_0/\langle X \rangle$ defines the static stiffness. Moreover, Eq. **15** implies that the dissipation coefficient $\omega\tilde{\chi}''(\omega)$ is always positive, for $\tilde{C} > 0$. As required by the second law of thermodynamics, a passive system thus cannot, on average, extract thermal energy from the environment.

If the system is removed from equilibrium by an energy-consuming mechanism, the FDT no longer holds. In this case, active events with unknown correlations add to thermal fluctuations, so no general relation links the autocorrelation of the system's spontaneous fluctuations to its responsiveness to small external stimuli. As a measure of the degree of violation of the FDT, we introduce the ratio

$$\frac{T_{\mathrm{EFF}}(\omega)}{T} = \frac{\omega\tilde{C}(\omega)}{2\,k_B T\tilde{\chi}''(\omega)}, \qquad [17]$$

which defines an effective temperature, $T_{\mathrm{EFF}}(\omega)$. $T_{\mathrm{EFF}}(\omega)$, which can be either positive or negative, is the temperature for which the FDT would be satisfied at angular frequency ω. In a passive system, $T_{\mathrm{EFF}}(\omega)$ must be identical to the ambient temperature; the ratio in Eq. **17** is then unity at all frequencies. If $T_{\mathrm{EFF}}(\omega)$ departs from the ambient temperature at some frequencies, however, the system cannot be at thermal equilibrium but must be actively driven.

Hair-Bundle Response to Mechanical Stimulation. By imposing sinusoidal movements at the stimulus fiber's base, we applied periodic forces at a hair bundle's tip. We chose displacement amplitudes small enough to maintain the bundle in a regime of linear responsiveness (27). For an oscillating bundle, this amplitude was typically 15 nm or less. We measured the linear response function, $\tilde{\chi}(\omega)$, at various frequencies near the frequency of spontaneous bundle oscillation, ν_0.

The real part of the response function, $\tilde{\chi}'(\omega)$, describes the elastic component of the bundle's response. Everywhere positive, it peaked at a frequency near ν_0 before declining to a plateau at higher frequencies (Fig. 2*A*). The plateau corresponded to a hair-bundle stiffness of $\sim$1 mN·m^{-1}, a value typical of the static bundle stiffness in the bullfrog's sacculus (24, 31). As a control, we also measured the response function of a hair cell that did not exhibit pronounced spontaneous oscillation. This cell showed a slowly declining elastic response that coincided at high frequencies with the plateau in the response of the oscillatory cell.

The imaginary part of the response function, $\tilde{\chi}''(\omega)$, reflects the work provided by the external stimulus to the combination of the bundle and fiber. For a passive system, this work must be of positive sign at all frequencies to balance viscous dissipation caused by the system's movement through the surrounding fluid. The striking feature of our measurement is that $\tilde{\chi}''(\omega)$ changed its sign at a frequency near ν_0 (Fig. 2*B*), indicating that energy was on average withdrawn from the hair bundle at frequencies below ν_0. Note that the change in sign of $\tilde{\chi}''(\omega)$ corresponds to a change in sign of the phase difference between stimulus and response (21). In the case of the control cell, $\tilde{\chi}''(\omega)$ displayed a positive sign at all frequencies and increased proportionally with frequency (Fig. 2*B*).

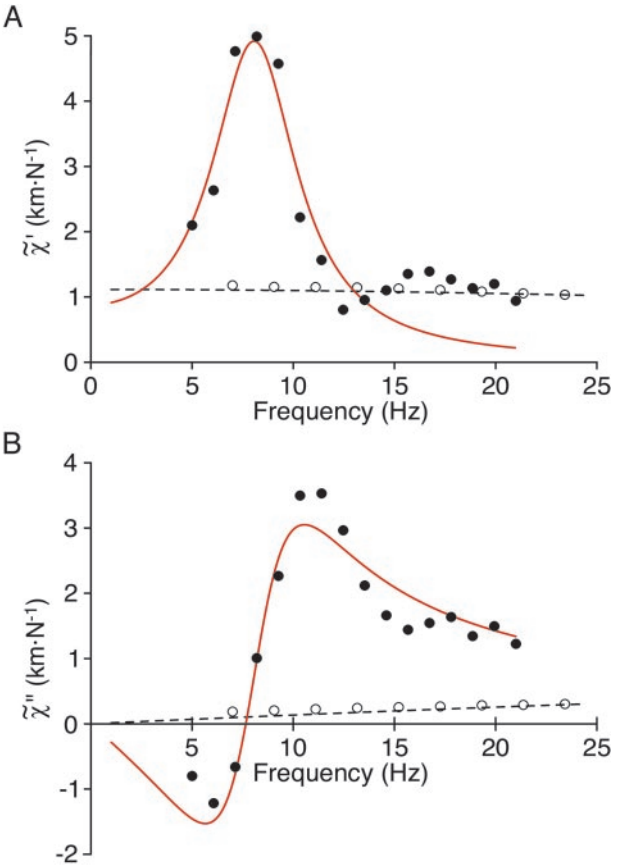

Fig. 2. Linear response function as a function of stimulus frequency for an oscillatory hair bundle (●) and a control bundle that did not show marked oscillations (○). (*A*) In the case of the oscillating hair bundle, the real part of the response function, $\tilde{\chi}'(\omega)$, which measures the bundle's elastic component of the response, shows a distinct peak near 8 Hz, the bundle's frequency of spontaneous oscillation. (*B*) The imaginary part of the response function, $\tilde{\chi}''(\omega)$, portrays the dissipative component of motion. For the oscillating bundle of Fig. 1, this crosses the abscissa at a frequency near that of the bundle's spontaneous oscillations. From the fits of the measured response function $\tilde{\chi}(\omega)$ by Eq. **20**, we found for the oscillatory bundle (smooth curve) $\lambda = 6.5$ μN·s·m^{-1}, $k = 104$ μN·m^{-1}, and $\nu_0 = \omega_0/(2\pi) = 8.1$ Hz. These values imply that $k = 1040$ μN·m^{-1} and provide a relaxation time for bundle motion of $\tau = 65$ ms. Applied to the control cell, the same model yielded (dotted line) $\lambda = 1.7$ μN·s·m^{-1}, $k = 900$ μN·m^{-1}, and $\nu_0 = \omega_0/(2\pi) \approx 0$ Hz; the corresponding relaxation time was $\tau = 2$ ms. The bundle's response function was measured by applying a succession of 50-cycle stimuli of increasing frequency separated by 2-s rests; the amplitude of stimulation was 15 nm for the oscillatory cell and 300 nm for the control cell. The periods during which the bundle was not stimulated were used to compute the characteristics of the bundle's spontaneous motion shown in Fig. 1.

Effective Temperature of the Hair Bundle. We calculated at each frequency the effective temperature, $T_{\mathrm{EFF}}(\omega)$, at which the observed movements would have satisfied the FDT (Eq. **17**). $T_{\mathrm{EFF}}(\omega)$ departed from the actual temperature, T, at all measured frequencies (Fig. 3 *A* and *B*). The degree of violation of the FDT, as measured by the ratio $T_{\mathrm{EFF}}(\omega)/T$, depended on frequency. In keeping with the behavior of the imaginary part of the hair bundle's response function (Fig. 2*B*), $T/T_{\mathrm{EFF}}(\omega)$ crossed the abscissa and changed its sign near the hair bundle's frequency of spontaneous oscillation (Fig. 3*A*). $T_{\mathrm{EFF}}(\omega)/T$ thus displayed a divergence before reaching a value of $\sim$4 at the greatest frequencies measured (Fig. 3*B*). The hair bundle therefore violated the FDT at all frequencies explored here.

For a hair bundle without striking spontaneous oscillations,

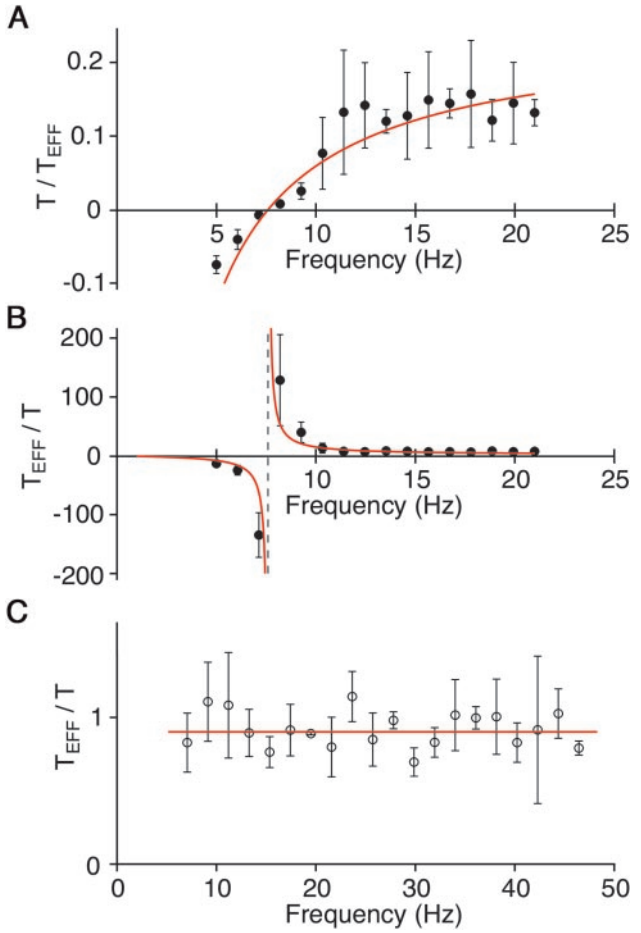

Fig. 3. The effective temperature of spontaneous hair-bundle motion. (*A*) For the oscillatory bundle of Figs. 1 and 2, the inverse of the effective temperature, normalized by the actual temperature, $T/T_{\mathrm{EFF}}(\omega)$, crossed zero near the bundle's frequency of spontaneous oscillation. This ratio deviated strikingly at all frequencies from the value of unity indicative of passive motion and thus violated the FDT. (*B*) A plot of the normalized effective temperature, $T_{\mathrm{EFF}}(\omega)/T$, exhibits a divergence corresponding to the crossing of the abscissa in *A*. The smooth lines correspond to a fit to the data by Eq. **22**. (*C*) For the control hair bundle whose response function is shown by open symbols in Fig. 2, the normalized effective temperature $T_{\mathrm{EFF}}(\omega)/T$ remained near unity throughout the range of frequencies. This behavior, which satisfies the FDT, demonstrated that the hair bundle was passive and that its fluctuations resulted from thermal bombardment.

the effective temperature obtained from the autocorrelation and the response function satisfied $T_{\mathrm{EFF}}(\omega)/T \cong 1$ for all observed frequencies (Fig. 3*C*). The spontaneous movements of this hair bundle were therefore thermal fluctuations.

Discussion

Violation of the FDT by an oscillating hair bundle demonstrates that both the hair bundle's spontaneous motion and its response to sinusoidal stimulation are active phenomena, governed by a process that requires a cellular energy source and that can do work. The observation that hair-bundle oscillations are not phase-coherent indicates that fluctuations play an important role in this process. The observed autocorrelation function does not reveal specific properties of the active process. The linear response function, however, provides insight into the underlying mechanism. The imaginary part of the response function crossed zero near the spontaneous oscillation frequency, whereas the real part remained positive at all frequencies. Only a certain class of active oscillators exhibits this behavior. In particular, the van der Pol oscillator, a standard model that generates spontaneous oscillations by introducing negative friction, behaves differently. In this case, the real part of the corresponding response function crosses zero, whereas the imaginary part does not change sign. Our observations thus rule out the hypothesis (5) that the active process generates a force proportional to velocity, which negates friction.

Model for Noisy Oscillations. We may describe the linear behavior of hair-bundle deflections by the equation

$$\lambda \frac{dX(t)}{dt} = -kX(t) + F_A(t) + f(t) + \eta_X(t), \qquad [18]$$

in which λ is an effective drag coefficient, k an effective stiffness, and $f(t)$ an external force. An active process within the hair bundle generates the force $F_A(t)$. As discussed below, $F_A(t)$ obeys the relation

$$\beta \frac{dF_A(t)}{dt} = -\bar{k}X(t) - F_A(t) + \eta_A(t). \qquad [19]$$

Here β is the relaxation time of the active process and the stiffness $\bar{k}$ characterizes the coupling of active elements to hair-bundle displacements. The random forces, $\eta_X(t)$ and $\eta_A(t)$, account for the effect of fluctuations on the bundle position and the active process, respectively.

We fitted the response functions calculated from this model to the experimentally measured linear response functions (Fig. 2). This fit yielded $\beta \approx \lambda/k$, a result that suggests that the hair bundle's position relaxes with a time constant similar to that of the bundle's force-producing elements. If we impose the condition that $\beta = \lambda/k$, the linear response function assumes the form

$$\tilde{\chi}(\omega) = \frac{1/2}{i\lambda(\omega_0 - \omega) + k} + \frac{1/2}{-i\lambda(\omega_0 + \omega) + k}, \qquad [20]$$

in which $\omega_0 = (k\bar{k})^{1/2}/\lambda$ is the angular frequency of oscillation. Furthermore, the autocorrelation function of spontaneous displacements in this simple model obeys the relation

$$\tilde{C}(\omega) = \frac{D}{k^2 + \lambda^2(\omega - \omega_0)^2} + \frac{D}{k^2 + \lambda^2(\omega + \omega_0)^2}, \qquad [21]$$

in which we have assumed symmetrical, δ-correlated noise: $\langle \eta_X(t)\eta_X(0)\rangle = \langle \eta_A(t)\eta_A(0)\rangle = 2D\delta(t)$. The correlation time of the oscillation is thus $\tau = \beta = \lambda/k$. For $\omega > 0$ and $\omega_0 \gg \tau^{-1}$, we may ignore the final terms of Eqs. **21** and **22** and approximate the effective temperature as

$$\frac{T_{\mathrm{EFF}}(\omega)}{T} \cong \frac{D}{\lambda k_{\mathrm{B}} T}\left(\frac{\omega}{\omega - \omega_0}\right). \qquad [22]$$

This model is in qualitative agreement with the data. In particular, $T_{\mathrm{EFF}}(\omega)/T$ diverges and changes sign when $\omega \approx \omega_0$ (Fig. 3). Also as observed, $T_{\mathrm{EFF}}(\omega)/T$ reaches a constant value at high frequencies. Near the frequency of spontaneous oscillation for the active hair bundle, the fit of the response function by Eq. **20** yields an effective bundle stiffness of $k \approx 100\ \mu\mathrm{N{\cdot}m^{-1}}$. As a result of the active process, this bundle appears to be almost one order of magnitude more compliant, and therefore more responsive, than the passive bundle. Probably because active elements within the oscillatory bundle create internal friction, the bundle's effective drag coefficient is $\lambda \approx 6.6\ \mu\mathrm{N{\cdot}s{\cdot}m^{-1}}$, about thrice that of the passive bundle. These parameter values yield a relaxation time of $\tau = \lambda/k \approx 65$ ms. The elastic coupling between force-generating elements and the hair-bundle position

is characterized by a stiffness of $\bar{k} \approx 1$ mN·m^{-1}. Finally, the fit of the oscillatory bundle's spectrum to Eq. **21** provides estimates for the noise strength of $D \approx 0.14$ pN^2·s and for the correlation time of 115 ms. A fit to the passive bundle's spectrum yields a noise strength only 2% as large (not shown). The discrepancy between correlation and relaxation times may result from the simplistic assumption that the hair bundle is subjected to symmetrical white noise. The bimodal shape of the displacement histogram (Fig. 1*B*) is consistent with the measurement of a bare negative stiffness in a displacement-clamp configuration (22) but is not accommodated by a linear description.

Active Elements in the Hair Bundle. What might be the physical origin of the active force described by Eqs. **18** and **19**? The myosin-based molecular motor responsible for a bundle's mechanical adaptation to sustained stimuli (reviewed in refs. 32–34) is an obvious candidate for one force-generating element within the hair bundle. The interplay between the adaptation motor and a region of negative stiffness in the force-displacement relation of a hair bundle could explain the oscillations (22). When acting against elastic elements, groups of molecular motors are also known to be able to generate oscillations by collective effects (35). In response to a step displacement of the hair bundle's tip, the speed of adaptation declines exponentially, and its initial value increases linearly with the deflection amplitude over the range of stimulation relevant to the present study (36). This behavior can be summarized by the equation $\beta dX_A(t)/dt = -X_A(t) + (\bar{k}/\mathrm{K})X(t)$, in which $X_A(t)$ denotes a displacement that can be related by a geometric factor to the movement of the adaptation motor. Expressing the force exerted by these motors on the hair bundle as $F_A = -\mathrm{K}X_A$, in which K represents a stiffness that couples the adaptation motor to hair-bundle motion, we obtain Eq. **19**.

Rapid transduction-channel reclosure mediated by Ca^{2+} binding to these channels could contribute to spontaneous hair-bundle oscillations as well as to the movements evoked by mechanical stimulation (20, 24, 37; reviewed in refs. 14, 16). Theoretical analysis shows that this process can both amplify mechanical stimuli and produce spontaneous bundle oscillations (8).

Proximity to a Hopf Bifurcation. An active oscillator such as a hair bundle may operate near an oscillatory instability called a Hopf bifurcation. In the absence of noise, the oscillator would be quiescent on one side of the bifurcation and display phase-coherent oscillations on the other. The distance to the Hopf bifurcation can be characterized by the inverse correlation time of the system's spontaneous movements, τ^{-1}, which vanishes at the instability and formally becomes negative on the unstable side of the bifurcation. Note that in our model, this bifurcation occurs when the effective stiffness k vanishes (see Eq. **21**). In our experiments, a bundle's spontaneous movements displayed a finite correlation time, corresponding to a positive effective stiffness k, and lost their phase coherence within one cycle of oscillation (Fig. 1*D*). This loss of coherence implies that the hair bundle is a noisy system. In the presence of noise, spontaneous motion exists on the stable side of the bifurcation, and the phase coherence of oscillations on the oscillating side is lost. As a result, the strict distinction between the oscillating and nonoscillating states ceases to exist; the Hopf bifurcation is concealed by the noise, but its signature (27)—frequency selectivity and compressive nonlinearity—remains.

The noise examined here results from both thermal impulses and fluctuations in force-producing elements within the hair bundle, including adaptation motors and transduction channels whose numbers are relatively small (reviewed in ref. 32). When operating in the vicinity of a noisy Hopf bifurcation, a hair bundle may benefit from noise in the detection of weak sinusoidal stimuli (9). Minute stimuli at a frequency near that of spontaneous oscillation partially phase-lock the bundle's movements, even though they are too weak to augment their magnitude. In the present study, we have explored only the linear response of the system to weak stimuli. For stronger stimulation, the system exhibits a compressive nonlinearity that allows it to operate over a large dynamic range (27).

We thank Drs. J. Prost, M. Magnasco, E. Siggia, and A. Libchaber for stimulating discussions and Mr. B. Fabella for computer programming. Dr. T. Duke and the members of our research group provided valuable comments on the manuscript. This investigation was supported by National Institutes of Health Grant DC00241. During the initial phase of the project, P.M. was an Associate of the Howard Hughes Medical Institute, of which A.J.H. remains an Investigator.

1. Probst, R. (1990) *Adv. Otorhinolaryngol.* **44,** 1–91.
2. Manley, G. A. & Köppl, C. (1998) *Curr. Opin. Neurobiol.* **8,** 468–474.
3. Manley, G. (2000) *Proc. Natl. Acad. Sci. USA* **97,** 11736–11743.
4. Ruggero, M. A., Kramek, B. & Rich, N. C. (1984) *Hear. Res.* **13,** 293–296.
5. Gold, T. (1948) *Proc. R. Soc. London Ser. B* **135,** 492–498.
6. Ruggero, M. A. (1992) *Curr. Opin. Neurobiol.* **2,** 449–456.
7. Nilsen, K. E. & Russell, I. J. (2000) *Proc. Natl. Acad. Sci. USA* **97,** 11751–11758.
8. Choe, Y., Magnasco, M. O. & Hudspeth, A. J. (1998) *Proc. Natl. Acad. Sci. USA* **95,** 15321–15326.
9. Camalet, S., Duke, T., Jülicher, F. & Prost, J. (2000) *Proc. Natl. Acad. Sci. USA* **97,** 3183–3188.
10. Eguíluz, V. M., Ospeck, M., Choe, Y., Hudspeth, A. J. & Magnasco, M. O. (2000) *Phys. Rev. Lett.* **84,** 5232–5235.
11. Dallos, P. (1992) *J. Neurosci.* **12,** 4575–4585.
12. Nobili, R., Mammano, F. & Ashmore, J. (1998) *Trends Neurosci.* **21,** 159–167.
13. Ashmore, J. F., Géléoc, G. S. G. & Harbott, L. (2000) *Proc. Natl. Acad. Sci. USA* **97,** 11759–11764.
14. Hudspeth, A. J. (1997) *Curr. Opin. Neurobiol.* **7,** 480–486.
15. Hudspeth, A. J., Choe, Y., Mehta, A. D. & Martin, P. (2000) *Proc. Natl. Acad. Sci. USA* **97,** 11765–11772.
16. Fettiplace, R., Ricci, A. J. & Hackney, C. M. (2001) *Trends Neurosci.* **24,** 169–175.
17. Crawford, A. C. & Fettiplace, R. (1985) *J. Physiol.* **364,** 359–379.
18. Howard, J. & Hudspeth, A. J. (1987) *Proc. Natl. Acad. Sci. USA* **84,** 3064–3068.
19. Denk, W. & Webb, W. W. (1992) *Hear. Res.* **60,** 89–102.
20. Benser, M. E., Marquis, R. E. & Hudspeth, A. J. (1996) *J. Neurosci.* **16,** 5629–5643.
21. Martin, P. & Hudspeth, A. J. (1999) *Proc. Natl. Acad. Sci. USA* **96,** 14306–14311.
22. Martin, P., Mehta, A. D. & Hudspeth, A. J. (2000) *Proc. Natl. Acad. Sci. USA* **97,** 12026–12031. (First Published October 10, 2000; 10.1073/pnas.210389497)
23. Denk, W., Webb, W. W. & Hudspeth, A. J. (1989) *Proc. Natl. Acad. Sci. USA* **86,** 5371–5375.
24. Howard, J. & Hudspeth, A. J. (1988) *Neuron* **1,** 189–199.
25. Russell, I. J., Kössl, M. & Richardson, G. P. (1992) *Proc. R. Soc. London Ser. B* **250,** 217–227.
26. Géléoc, G. S. G., Lennan, G. W. T., Richardson, G. P. & Kros, C. J. (1997) *Proc. R. Soc. London Ser. B* **264,** 611–621.
27. Martin, P. & Hudspeth, A. J. (2001) *Proc. Natl. Acad. Sci. USA* **98,** 14386–14391. (First Published November 27, 2001; 10.1073/pnas.251530498)
28. Bialek, W. & Wit, H. P. (1984) *Phys. Lett. A* **104,** 173–178.
29. Bialek, W. (1987) *Annu. Rev. Biophys. Biophys. Chem.* **16,** 455–478.
30. Doi, M. & Edwards, S. F. (1986) *The Theory of Polymer Dynamics* (Oxford Science Publications, Oxford, U.K.), pp. 58–62.
31. Marquis, R. E. & Hudspeth, A. J. (1997) *Proc. Natl. Acad. Sci. USA* **94,** 11923–11928.
32. Hudspeth, A. J. & Gillespie, P. G. (1994) *Neuron* **12,** 1–9.
33. Eatock, R. A. (2000) *Annu. Rev. Neurosci.* **23,** 285–314.
34. Holt, J. R. & Corey, D. P. (2000) *Proc. Natl. Acad. Sci. USA* **97,** 11730–11735.
35. Jülicher, F. & Prost, J. (1997) *Phys. Rev. Lett.* **78,** 4510–4513.
36. Hacohen, N., Assad, J. A., Smith, W. J. & Corey, D. P. (1989) *J. Neurosci.* **9,** 3988–3997.
37. Ricci, A. J., Crawford, A. C. & Fettiplace, R. (2000) *J. Neurosci.* **20,** 7131–7142.